

A qRT-PCR and Gene Functional Enrichment Study Focused on Downregulation of miR-141-3p in Hepatocellular Carcinoma and Its Clinicopathological Significance

Technology in Cancer Research & Treatment
 2017, Vol. 16(6) 835–849
 © The Author(s) 2017
 Reprints and permission:
sagepub.com/journalsPermissions.nav
 DOI: 10.1177/1533034617705056
journals.sagepub.com/home/tct


Cui-zhen Liu, MD^{1,#}, Zhi-hua Ye, MD^{2,#}, Jie Ma, PhD, MD¹,
 Rong-quan He, MD¹, Hai-wei Liang, MD¹, Zhi-gang Peng, PhD, MD¹,
 and Gang Chen, PhD, MD²

Abstract

Background: The clinical significance of miR-141-3p in hepatocellular carcinoma has not been verified. Therefore, we conducted this study to examine miR-141-3p expression and its clinical significance in hepatocellular carcinoma and to investigate the functions of its potential targets. **Methods:** The Cancer Genome Atlas database and the Gene Expression Omnibus database were used to explore the aberrant expression of miR-141-3p in hepatocellular carcinoma. Furthermore, we assessed the miR-141-3p levels in 95 hepatocellular carcinoma tissues with 95 matched adjacent tissues using real-time quantitative polymerase chain reaction. Moreover, a target gene prediction analysis of miR-141-3p, a natural language processing analysis for hepatocellular carcinoma using PubMed, and a gene functional enrichment analysis were conducted to search the potential function of miR-141-3p in the pathogenesis of hepatocellular carcinoma. **Results:** Regarding The Cancer Genome Atlas data, miR-141-3p levels were markedly downregulated in hepatocellular carcinoma tissue compared to para- or nontumor tissue (4.6112 [1.7096] vs 5.3053 [1.4254], $P = .045$). MiR-141-3p expression was reduced in patients with hepatocellular carcinoma with a low pathologic T stage ($P = .006$), a low grade ($P = .01$), elderly hepatocellular carcinoma patients ($P = .001$), and male patients with hepatocellular carcinoma ($P = .01$) compared with that in patients with hepatocellular carcinoma with high pathologic T stages, high grades, young patients with hepatocellular carcinoma, and female patients with hepatocellular carcinoma. However, according to the Gene Expression Omnibus database, no significant differences in the expression of miR-141-3p were observed between hepatocellular carcinoma tissue and normal liver tissue ($P = .984$). Real-time quantitative polymerase chain reaction confirmed a similar trend of decreased miR-141-3p in hepatocellular carcinoma tissue (1.7542 [0.8663] vs 2.5562 [1.7913], $P = .001$) as observed in The Cancer Genome Atlas. In addition, decreased miR-141-3p levels were detected in the multiple tumor nodes group ($P = .004$), the metastasis group ($P < .001$), and the advanced TNM stage group ($P = .01$), compared to the single tumor nodes group, the nonmetastasis group, and the early TNM stage group. Two hundred eighty-two genes were identified from the overlap between the predicted targets and the natural language processing analysis. Gene ontology and Kyoto Encyclopedia of Genes and Genomes pathway analyses revealed several significant biological functions and pathways related to the pathogenesis of

¹ Department of Medical Oncology, First Affiliated Hospital of Guangxi Medical University, Nanning, Guangxi Zhuang Autonomous Region, People's Republic of China

² Department of Pathology, First Affiliated Hospital of Guangxi Medical University, Nanning, Guangxi Zhuang Autonomous Region, People's Republic of China

Cui-zhen Liu and Zhi-hua Ye have contributed equally to this article.

Corresponding Authors:

Zhi-gang Peng, PhD, MD, Department of Medical Oncology, First Affiliated Hospital of Guangxi Medical University, Shuangyong Road 6, Nanning, Guangxi Zhuang Autonomous Region 530021, People's Republic of China.
 Email: drpzg001@163.com

Gang Chen, PhD, MD, Department of Pathology, First Affiliated Hospital of Guangxi Medical University, No. 6 Shuangyong Road, Nanning, Guangxi Zhuang Autonomous Region 530021, People's Republic of China.
 Email: chen_gang_triones@163.com



cancers, including hepatocellular carcinoma. **Conclusion:** Downregulation of miR-141-3p might be responsible for the carcinogenesis and aggressiveness of hepatocellular carcinoma. MiR-141-3p may act as an antitumor microRNA, which is essential for hepatocellular carcinoma progression through the regulation of various signaling pathways. Thus, interactions with miR-141-3p may provide a novel strategy for hepatocellular carcinoma treatment in the future.

Keywords

miR-141-3p, hepatocellular carcinoma, qRT-PCR, target genes, gene functional enrichment analysis

Abbreviations

GEO, Gene Expression Omnibus; GO, gene ontology; HCC, hepatocellular carcinoma; KEGG, Kyoto Encyclopedia of Genes and Genomes; NLP, natural language processing; qRT-PCR, real-time quantitative polymerase chain reaction; SMD, standard mean difference; TCGA, The Cancer Genome Atlas

Received: October 16, 2016; Revised: March 03, 2017; Accepted: March 20, 2017.

Introduction

Hepatocellular carcinoma (HCC), a common malignancy in China, has an increased incidence and a poor prognosis.^{1,2} Over the past few decades, great progress has been made in the treatment of HCC, including surgery, interventional therapy, radiotherapy, chemotherapy, and molecular target treatment. However, the prognosis of HCC is still unfavorable.^{3,4} Therefore, it is necessary to identify highly stable and specific molecular targets to facilitate early diagnosis of HCC and allow targeted therapy to improve the prognosis of HCC.

MicroRNAs (miRNAs), which are approximately 22 nucleotides in length, belong to a large family of noncoding, single-stranded RNAs. Increasing evidence indicates that miRNAs participate in cell growth, apoptosis, and cell proliferation.^{5,6} It has been reported that miRNAs contribute to carcinogenesis and the progression of cancers by positive or negative regulation of the hub genes involved in the pathogenesis of cancers.^{7,8} Two studies have demonstrated a downregulation of miR-141-3p expression in HCC tissues.^{9,10} However, these 2 studies have several limitations—unmatched analysis of miR-141-3p expression in HCC and limited sample size, which may lead to a false-positive conclusion. Therefore, it is necessary to validate the aberrant expression of miR-141-3p in HCC tissue with a matched analysis to eliminate the unrelated parameters.

In this current study, we examined the miR-141-3p level in HCC and its clinical significance for the diagnosis and prediction of prognosis in HCC. Moreover, the prospective mechanisms of the pathogenesis of HCC were analyzed by identifying the potential target genes of miR-141-3p and performing a gene functional enrichment analysis.

Materials and Methods

Patients and Samples

We selected 95 patients with HCC and matched adjacent nontumor tissues from 75 men and 20 women with a mean

age of 50. The patients had not received any adjuvant therapy before undergoing surgery between March 2010 and March 2012 at the First Affiliated Hospital of Guangxi Medical University. There were 22 patients with HCC in early TNM stage (I+II) and 73 patients in advanced TNM stage (III+IV). Forty-nine cases existed metastasis, 32 cases had portal vein tumor embolus, 36 cases had vaso-invasion, and 50 cases achieved cirrhosis. Two pathologists independently confirmed all of the pathological diagnoses, and we gained the approval of the use of the patients' tissue samples for this study.

MiR-141-3p Expression in HCC in The Cancer Genome Atlas

The Cancer Genome Atlas (TCGA) database was used to examine miR-141-3p expression in HCC tissues. In addition, miR-141-3p expression in patients with HCC with various clinicopathological characteristics was also analyzed. In TCGA database, level 3 data of the miRNA profile of HCC were extracted. Meanwhile, the corresponding clinical data for HCC were obtained. Afterward, the miR-141-3p expression was extracted from the miRNA profile, and statistical analyses were conducted to estimate the expression of miR-141-3p in HCC and to explore the relationships between miR-141-3p expression and various clinicopathological factors.

MiR-141-3p Expression in HCC in the Gene Expression Omnibus

In the Gene Expression Omnibus (GEO) database including the GEO data set and GEO profile, we searched for miR-141-3p expression in HCC using the following key words: (1) hepatocellular OR liver OR hepatic OR HCC, (2) malignan* OR cancer OR tumor OR tumour OR neoplas* OR carcinoma, and (3) microRNA OR miRNA OR miR. The microarrays were included to examine miR-141-3p expression in HCC tissues and noncancerous tissues and to explore

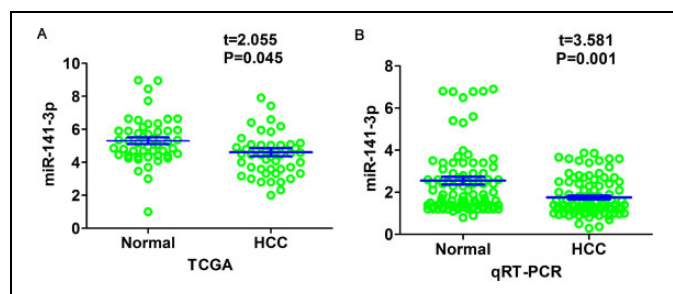


Figure 1. MiR-141-3p expression in HCC tissues and nontumor liver tissues. A, A comparison of miR-141-3p levels in 49 HCC tissues and 49 nontumor tissues in the TCGA database. $P = .045$. The expression level of miR-141-3p in TCGA data was normalized using a logarithm. B, A comparison of miR-141-3p levels in 95 pairs of HCC tissues and adjacent nontumor tissues using qRT-PCR. $P < .001$. HCC indicates hepatocellular carcinoma; qRT-PCR, real-time quantitative polymerase chain reaction; TCGA, The Cancer Genome Atlas.

miR-141-3p expression in different clinicopathological features of HCC.

A meta-analysis was performed with Stata version 12.0, which combined the miR-141-3p expression data from the real-time quantitative polymerase chain reaction (qRT-PCR), the microarray data of the GEO database, and the RNA sequencing data of the TCGA database in different tissues. Standard mean difference (SMD) and a 95% confidence interval (95% CI) were used to assess miR-141-3p expression in different tissues. Moreover, a Q test (χ^2 test) and I^2 statistics were performed to estimate the heterogeneity among the eligible studies. A Mantel-Haenszel fixed-effects model was performed if no obvious heterogeneity exists among the pooled studies ($I^2 < 50\%$ and $P > .1$). However, a random-effects model was

utilized when obvious heterogeneity was observed among the studies ($I^2 > 50\%$ or $P < .1$).¹¹

Real-Time Quantitative Polymerase Chain Reaction

The qRT-PCR protocol has been described previously. A combination of RUN6B and RUN48, which has been shown to be a stable internal control in our previous studies, was used as a reference to detect miR-141-3p levels.¹²⁻¹⁴ The RNU6B, RNU48, and miR-141-3p primers were included in the TaqMan MicroRNA assays (4427975, Applied Biosystems, Life Technologies, Grand Island, New York), and their sequences are as follows: miR-141-3p, UAACACUGUCUGUAAAGAUGG; RNU6B, CGCAAGGAUGACACGCAAUUCGUGAAGC-GUCCAUAUUUUU; RNU48, GAUGACCCCAGGUAA-CUCUGAGUGUGUCGUGAUGCCAUCACCGCAGCG-CUCUGACC. The expression level of miR-141-3p was calculated by formula $2^{-\Delta\Delta q}$.

MicroRNA Target Prediction

Twelve databases were used for the target prediction of miR-141-3p, including miRWalk, MicroT4, miRanda, mirbridge, miRDB, miRMap, miRNAMap, Pictar2, PITA, RNAhybrid, Targetscan, and miRWalk2.0.¹⁵ Three databases (miRecords, miRTarbase, and Tarbase) were searched for the validated targets of miR-141-3p. Next, further gene functional enrichment analysis was conducted on a combination of the predicted target genes of miR-141-3p that were reported in more than 4 databases and the validated genes of miR-141-3p that had strong evidence.

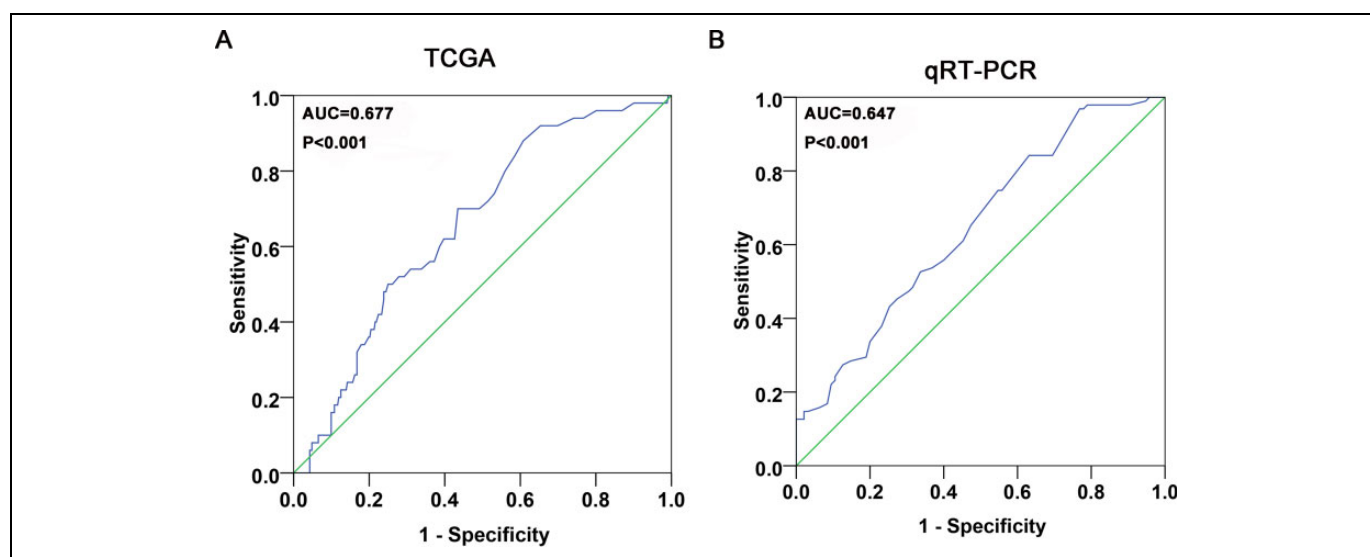


Figure 2. Diagnostic value of miR-141-3p in HCC. A, The ROC curve of miR-141-3p expression was used to assess its diagnostic value in HCC based on TCGA data. AUC = 0.677 (95% CI: 0.571-0.784, $P = .003$). B, The ROC curve of miR-141-3p expression by qRT-PCR was used to assess its diagnostic value in HCC. AUC = 0.647 (95% CI: 0.570-0.724, $P < .001$). AUC, area under the curve; HCC indicates hepatocellular carcinoma; ROC, receiver operating characteristic; qRT-PCR, real-time quantitative polymerase chain reaction.

Natural Language Processing Analysis of HCC-Related Studies

We searched the PubMed database with the following keywords: (1) hepatocellular OR liver OR hepatic OR HCC and (2) malignan* OR cancer OR tumor OR tumor OR neoplas* OR carcinoma. We extracted all of the related genes in the studies via using Biomedical Named Entity Recognizer (<http://pages.cs.wisc.edu/~bsettles/abner/>).

In the natural language processing (NLP) analysis, we counted the frequency of each gene that merged with the eligible studies in PubMed. A greater frequency indicated a higher likelihood of correlation between that particular gene and HCC. In PubMed, the total number of relevant studies was marked as “N,” the frequency of the related genes and HCC in PubMed was marked as “m” and “n,” and the simultaneous occurrence of the disease and a certain gene was marked as “k.” The probability of frequency greater than “k” cocitations was calculated with random conditions through hypergeometric distribution. A *P* value of less than .01 was considered statistically significant. The formula for the NLP analysis was as follows:

$$P = 1 - \sum_{i=0}^{k-1} p(i|n, m, N); p(i|n, m, N) = \frac{n!(N-n)!m!(N-m)!}{n-i!i!n-m!N-n-m+i!N!}$$

Gene Functional Enrichment Analysis

Gene ontology (GO), including biological process, molecular function, and cellular component, was conducted using DAVID (Database for Annotation, Visualization and Integrated Discovery) database.¹⁶ Cytoscape software (version: Cytoscape 3.3.0) and BINGO plugins were used to generate the graphical display of the GO network. The protein-to-protein network analysis was performed using STRING (version: STRING 10.0).¹⁷ The database of the Kyoto Encyclopedia of Genes and Genomes (KEGG) was also applied to reflect the prospective biological pathways of HCC which the targets of miR-141-3p were involved in.

Statistical Analysis

We performed the statistical analyses using SPSS version 22. We made use of mean (standard deviation [SD]) to present the quantitative data of miR-141-3p expression. Student *t* tests were performed for the analysis of miR-141-3p expression between 2 groups, and 1-way ANOVA (Analysis of Variance) was employed when more than 2 groups were analyzed. Additionally, we drew receiver operating characteristic (ROC) curves to measure the power of miR-141-3p in HCC diagnosis. Spearman analysis was also conducted to estimate the associations between miR-141-3p and clinical characteristics. A *P* < .05 was considered statistically different.

Table 1. Expression of miR-141-3p and Clinicopathological Parameters in HCC in TCGA.

| Clinicopathological Features | n | miR-141-3p Expression | | |
|------------------------------|-----------------|-----------------------|-------------------------------|----------|
| | | Mean (SD) | <i>t</i> | <i>P</i> |
| Tissue (unmatched) | | | | |
| Adjacent noncancerous liver | 50 | 5.3757 (1.4960) | 1.930 | .054 |
| HCC | 352 | 4.7907 (2.0666) | | |
| Tissue (matched) | | | | |
| Adjacent noncancerous liver | 49 ^a | 5.3053 (1.4254) | 2.055 | .045 |
| HCC | 49 | 4.6112 (1.7096) | | |
| Age | | | | |
| <60 | 162 | 5.1872 (2.3316) | 3.285 | .001 |
| ≥60 | 189 | 4.4542 (1.7512) | | |
| Gender | | | | |
| Male | 239 | 4.5736 (1.8064) | 2.595 | .01 |
| Female | 113 | 5.2501 (2.4773) | | |
| AJCC pathologic T | | | | |
| T1 | 174 | 4.4813 (1.4985) | 2.783 | .006 |
| T2-T4 | 175 | 5.0924 (2.4852) | | |
| AJCC pathologic N | | | | |
| N0 | 240 | 4.7649 (2.1709) | <i>F</i> = 0.225 ^b | .798 |
| N1 | 3 | 4.0876 (1.1607) | | |
| NX | 108 | 4.8438 (1.8377) | | |
| AJCC pathologic M | | | | |
| M0 | 255 | 4.8445 (2.2025) | <i>F</i> = 0.315 ^b | .730 |
| M1 | 4 | 4.7268 (1.4122) | | |
| MX | 93 | 4.6460 (1.6752) | | |
| Grade | | | | |
| I-II | 219 | 4.5681 (1.7138) | 2.596 | .01 |
| III-IV | 129 | 5.2140 (2.5009) | | |
| Cirrhosis | | | | |
| – | 328 | 4.7979 (2.0554) | 0.426 | .671 |
| + | 6 | 5.1569 (1.4361) | | |
| Pathologic stage | | | | |
| I-II | 245 | 4.6830 (1.8876) | 1.611 | .108 |
| III-IV | 82 | 5.1040 (2.4698) | | |
| Vaso-invasion | | | | |
| – | 195 | 4.6092 (1.8703) | 1.760 | .08 |
| + | 105 | 5.0549 (2.4153) | | |

Abbreviations: AJCC, American Joint Committee on Cancer; HCC, hepatocellular carcinoma; SD, standard deviation; TCGA, The Cancer Genome Atlas.

^aOnly 49 pairs were achieved for HCC tissues and corresponding matched adjacent noncancerous liver tissues because of missing data of miR-141-3p expression in a HCC tissue.

^bOne-way ANOVA (Analysis of Variance) analysis was performed.

Results

MiR-141-3p Expression in HCC Based on TCGA

Regarding TCGA data, lower miR-141-3p levels were detected in 352 HCC tissues compared to 50 adjacent normal liver tissues, but no statistic difference was gained (*P* = .054). However, when we matched the HCC tissues with corresponding adjacent normal liver tissues (49 pairs), significant downregulation of miR-141-3p levels was observed in HCC tissues

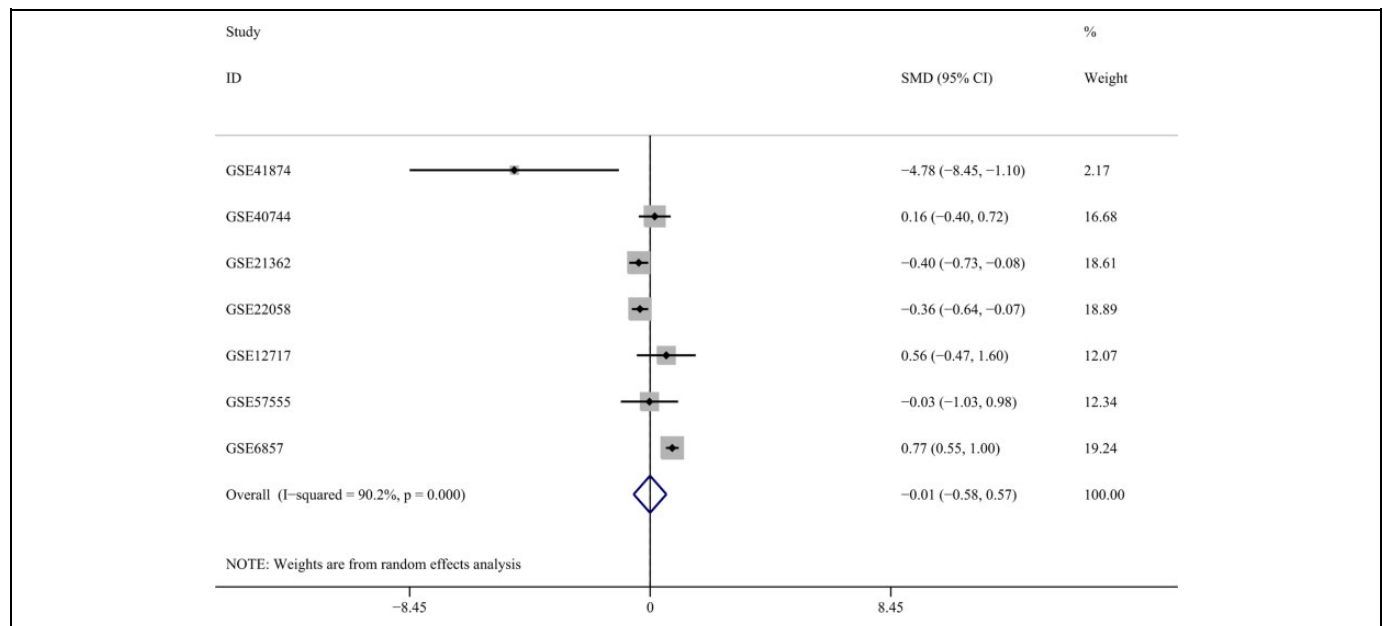


Figure 3. The forest plots of the meta-analysis of miR-141-3p expression in HCC using the GEO database. Seven studies were included in the GEO database, and the pooled SMD was -0.006 (95% CI: -0.580 to 0.569 , $P = .984$) with the random-effects model. CI indicates confidence interval; GEO, Gene Expression Omnibus; HCC hepatocellular carcinoma; SMD, standard mean difference.

(4.6112 [1.7096]), as compared to the adjacent normal liver tissues (5.3053 [1.4254], $P = .045$; Figure 1A). The P value of the diagnostic power was .003 (area under the curve [AUC] = 0.677, 95% CI: 0.571-0.784; Figure 2A). The relationships between miR-141-3p and the clinicopathological characteristics from TCGA are presented in Table 1.

Meta-Analysis of miR-141-3p Expression in HCC

Regarding the differences in miR-141-3p expression between HCC and nontumor liver tissues, 7 studies of microarrays in the GEO database (GSE41874, GSE40744, GSE21362, GSE22058, GSE12717, GSE57555, and GSE6857), which involved 353 HCC with 453 nontumor liver tissues, were included in this meta-analysis. The pooled SMD of miR-141-3p was -0.006 (95% CI: -0.580 to 0.569 , $P = .984$; Figure 3), and the P value of the heterogeneity test was $<.001$ ($I^2 = 90.2\%$).

MiR-141-3p Expression in HCC Detected by qRT-PCR and Its Clinicopathological Significance

In contrast to the adjacent normal liver tissue (2.5562 [1.7913]), miR-141-3p was significantly underexpressed in HCC tissue (1.7542 [0.8663], $P = .001$; Table 2, Figure 1B). Meanwhile, based on the ROC curve, the AUC was 0.647 (95% CI: 0.570-0.724, $P < .001$; Figure 2B).

All of the clinicopathological factors are shown in Table 2. Concerning the relationships between miR-141-3p and the clinicopathological characteristics in HCC tissues, we observed

lower expression in the multiple tumor nodes group (1.4795 [0.8120]) compared to the single tumor node group (1.9813 [0.8509], $P = .004$; Figure 4A). Meanwhile, miR-141-3p was expressed at lower levels in tissues with metastases (1.4392 [0.7227]) than in HCC tissues without metastases (2.0898 [0.8873], $P < .001$; Figure 4B). Moreover, in the III-IV clinical TNM stage group, miR-141-3p was also significantly down-regulated (1.6304 [0.8231]) compared to the stage I-II group (2.1650 [0.8978], $P < .001$, $P = .01$; Figure 4C). Furthermore, the HCC tissues with a portal vein tumor embolus had lower levels of miR-141-3p expression (2.2669 [1.1827]), while the tissues without a portal vein tumor embolus had higher expression levels of miR-141-3p (3.1146 [1.8511]) with a marginal P value of .05. The rest of clinicopathological characteristics of HCC had no significant correlation with miR-141-3p expression (Table 2).

In addition, Spearman analysis was used to assess the relationships between miR-141-3p and the clinicopathological parameters, and negative correlations were discovered between miR-141-3p and tumor nodes ($r = -.350$, $P = .001$), metastasis ($r = -.418$, $P < .001$), TNM ($r = -.343$, $P = .001$), or portal vein tumor embolus ($r = -.273$, $P = .007$). However, the correlations were relatively weak. No significant associations between the rest of the clinicopathological factors and miR-141-3p levels were noted.

Potential Target Genes of miR-141-3p

Twelve databases were searched to predict the potential targets of miR-141-3p. A total of 8201 genes were obtained from

Table 2. Expression of miR-141-3p and Clinicopathological Parameters in HCC in the 95 Pairs Detected by qRT-PCR.

| Clinicopathological Features | n | miR-141 Expression | | |
|------------------------------|----|--------------------|--------------------|----------|
| | | Mean (SD) | <i>t</i> | <i>P</i> |
| Tissue | | | | |
| Adjacent noncancerous liver | 95 | 2.5562 (1.7913) | 3.581 | .001 |
| HCC | 95 | 1.7542 (0.8663) | | |
| Age | | | | |
| ≥50 | 46 | 1.6280 (0.8034) | 1.382 | .170 |
| <50 | 49 | 1.8727 (0.9137) | | |
| Gender | | | | |
| Male | 75 | 1.6464 (0.7846) | 2.039 | .052 |
| Female | 20 | 2.1585 (1.0474) | | |
| Differentiation | | | | |
| High | 6 | 1.4333 (0.3882) | 0.541 ^a | .584 |
| Moderate | 60 | 1.7463 (0.7897) | | |
| Low | 29 | 1.8369 (1.0720) | | |
| Size | | | | |
| <5 cm | 18 | 1.6644 (0.8901) | 0.486 | .628 |
| ≥5 cm | 77 | 1.7752 (0.8652) | | |
| Tumor nodes | | | | |
| Single | 52 | 1.9813 (0.8509) | 2.921 | .004 |
| Multiple | 43 | 1.4795 (0.8120) | | |
| Metastasis | | | | |
| Without metastasis | 46 | 2.0898 (0.8873) | 3.904 | <.001 |
| With metastasis | 49 | 1.4392 (0.7227) | | |
| TNM stage | | | | |
| I-II | 22 | 2.1650 (0.8978) | 2.615 | .01 |
| III-IV | 73 | 1.6304 (0.8231) | | |
| Portal vein tumor embolus | | | | |
| - | 63 | 1.8779 (0.8268) | 1.984 | .05 |
| + | 32 | 1.5106 (0.9033) | | |
| Vaso-invasion | | | | |
| - | 59 | 1.8673 (0.8462) | 1.643 | .104 |
| + | 36 | 1.5689 (0.8786) | | |
| Cirrhosis | | | | |
| - | 45 | 1.6873 (0.8515) | 0.712 | .478 |
| + | 50 | 1.8144 (0.8836) | | |

Abbreviations: HCC, hepatocellular carcinoma; qRT-PCR, real-time quantitative polymerase chain reaction; SD, standard deviation.

^aOne-way ANOVA analysis was performed.

those databases, and 263 validated target genes were identified in a combination of the miRecords, miRTarbase, and Tarbase databases. Next, the genes reported in more than 4

databases were combined with the validated target genes, and finally, 2335 genes were selected to represent the targets of miR-141-3p. A flowchart of the prediction analysis was presented in Figure 5.

Overlap of the Predicted Target Genes of miR-141-3p, the NLP Analysis, and Its GO Analysis

In the NLP analysis, we extracted 1800 significant HCC-related genes. After combining them with the genes of the predicted targets and the validated target genes of miR-141-3p, 282 significant genes were identified, and they were used for further GO analysis. In this 282 identified targets of miR-141-3p in HCC, the Pearson correlative analysis revealed that the expression of 7 targets showed relatively higher negative correlation with miR-141-3p (CES2: $r = -.462$, MYRIP: $r = -.438$, PEBP1: $r = -.417$, BCKDHB: $r = -.313$, PPARA: $r = -.312$, GLYATL1: $r = -.312$, and IRS2: $r = -.306$, all $P < .001$; Figures 6 and 7). In the GO analysis, there were 489 significant terms involving biological processes ($P < .05$). Among them, we observed regulation of cell proliferation, the enzyme-linked receptor protein signaling pathway, the transmembrane receptor protein tyrosine kinase signaling pathway, and response to organic substance (Table 3). Moreover, there were 33 terms involving cellular components ($P < .05$), and some of them were associated with the membrane-enclosed lumen, organelle lumen, nucleoplasm, nuclear lumen, intracellular organelle lumen, and so on (Table 3). Meanwhile, there were 59 significant terms involving molecular functions ($P < .05$) including transmembrane receptor protein tyrosine kinase activity, protein tyrosine kinase activity, protein kinase activity, enzyme binding, and so on (Table 3).

Furthermore, we conducted BINGO analysis of the overlapping 282 genes from the predicted genes and validated target genes of miR-141-3p and the NLP. The results of the GO analysis are shown in Figures 8 to 10. In addition, a hub gene analysis was conducted using the protein-protein interactions, and the results are shown in Figure 11. In the network of the overlapping genes, several genes showed higher connectivity, including PTEN, SRC, PRKCA, PTGS2, and so on.

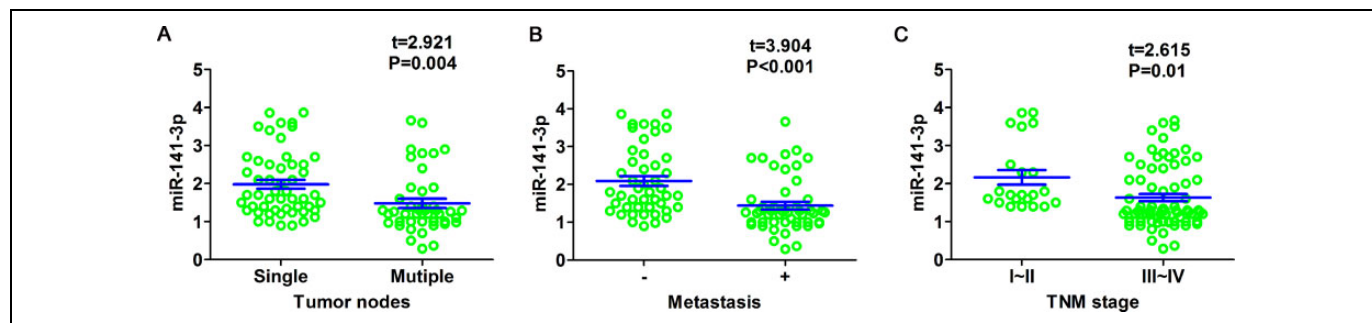


Figure 4. MiR-141-3p expression detected by qRT-PCR in various clinicopathological states of HCC. A, Tumor nodes. B, Metastasis. C, TNM stage. HCC indicates hepatocellular carcinoma; qRT-PCR, real-time quantitative polymerase chain reaction.

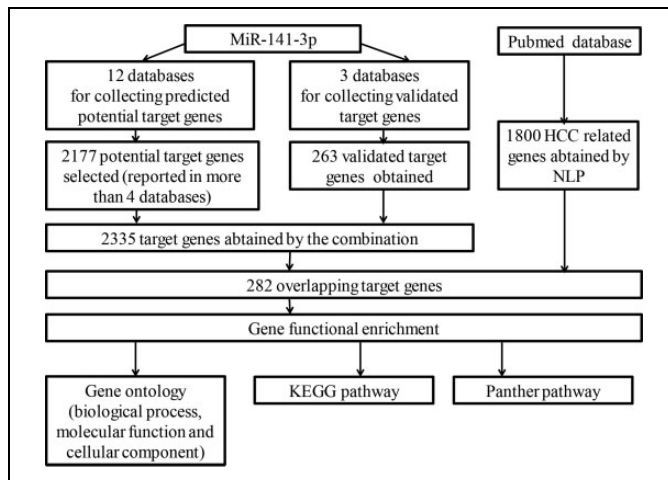


Figure 5. The flowchart of the gene functional enrichment.

Pathway Analysis of the Overlapping Genes Between the Predicted Genes, the Validated Target Genes of miR-141-3p, and the NLP in KEGG

The overlapping 282 genes between the predicted genes and the NLP were also used for pathway analysis in KEGG. There

were 39 available pathways, and 34 signaling pathways were selected ($P < .05$; Table 4) including pathways in cancer (FGFR1, E2F3, PTGS2, XIAP, GRB2, PDGFA, NFKBIA, KITLG, GLI2, PTEN, TGFB2, CCNE2, KRAS, ITGAV, AXIN1, EGFR, PRKCA, RET, CTBP2, RALBP1, MSH2, CBL, TGFB2, CYCS, CDK6, SMAD2, HGF, CTNNA1, CDK2, MAPK1, CRKL, CDKN1B, HDAC2, ITGA6, PDGFA, MAPK9, PDGFRB, PTCH1, $P = 1.45 \times 10^{-12}$), focal adhesion (PRKCA, E2F1, MAPK1, E2F3, BRAF, CDK6, CDK4, PTEN, AKT2, $P = 1.06E-05$), the ErbB signaling pathway (PRKCA, CDC42, MAPK1, CAV1, FLT1, BRAF, XIAP, CCND2, BCL2, ITGAV, RAC1, FIGF, PTEN, FN1, AKT2, $P = 1.18E-05$), the MAPK signaling pathway (PRKCA, E2F1, MAPK1, E2F3, BRAF, CDK6, CDK4, AKT2, $P = 1.88E-05$), the cell cycle (E2F1, MAPK1, E2F3, BRAF, CDK4, FIGF, MMP2, $P = 2.52E-05$), and so on (Table 4).

Pathway Analysis of the Overlapping Genes Between the Predicted Genes, the Validated Target Genes of miR-141-3p, and the NLP in Panther

In the Panther database, 16 available pathways were reported, and 13 signaling pathways were significant ($P < .05$) including several

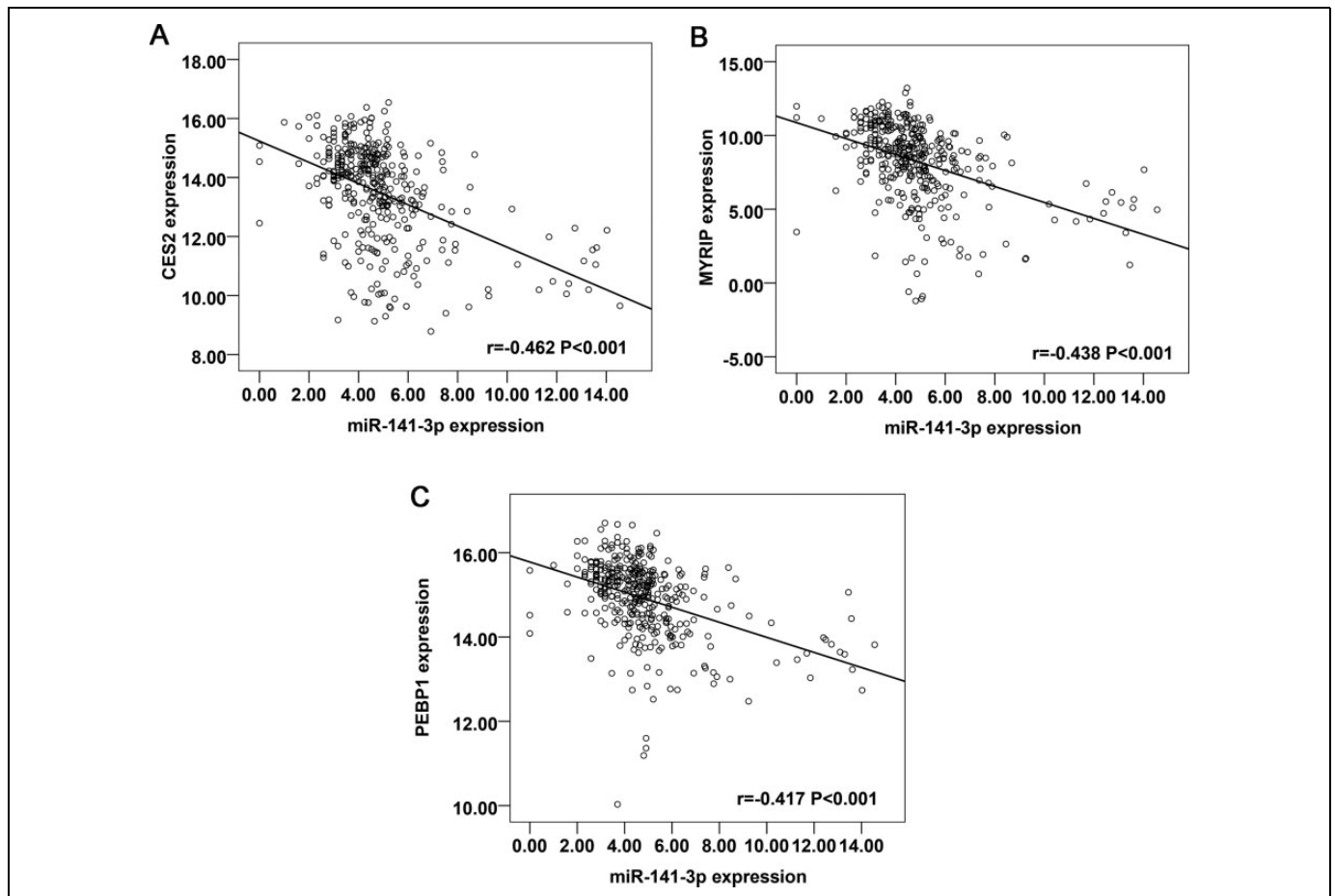


Figure 6. The correlation between miR-141-3p and 3 identified targets. A, CES2 ($r = -.462$, $P < .001$). B, MYRIP ($r = -.438$, $P < .001$). C, PEBP1 ($r = -.417$, $P < .001$). CES2, carboxylesterase 2; MYRIP, myosin VIIA and Rab interacting protein; PEBP1, phosphatidylethanolamine binding protein 1.

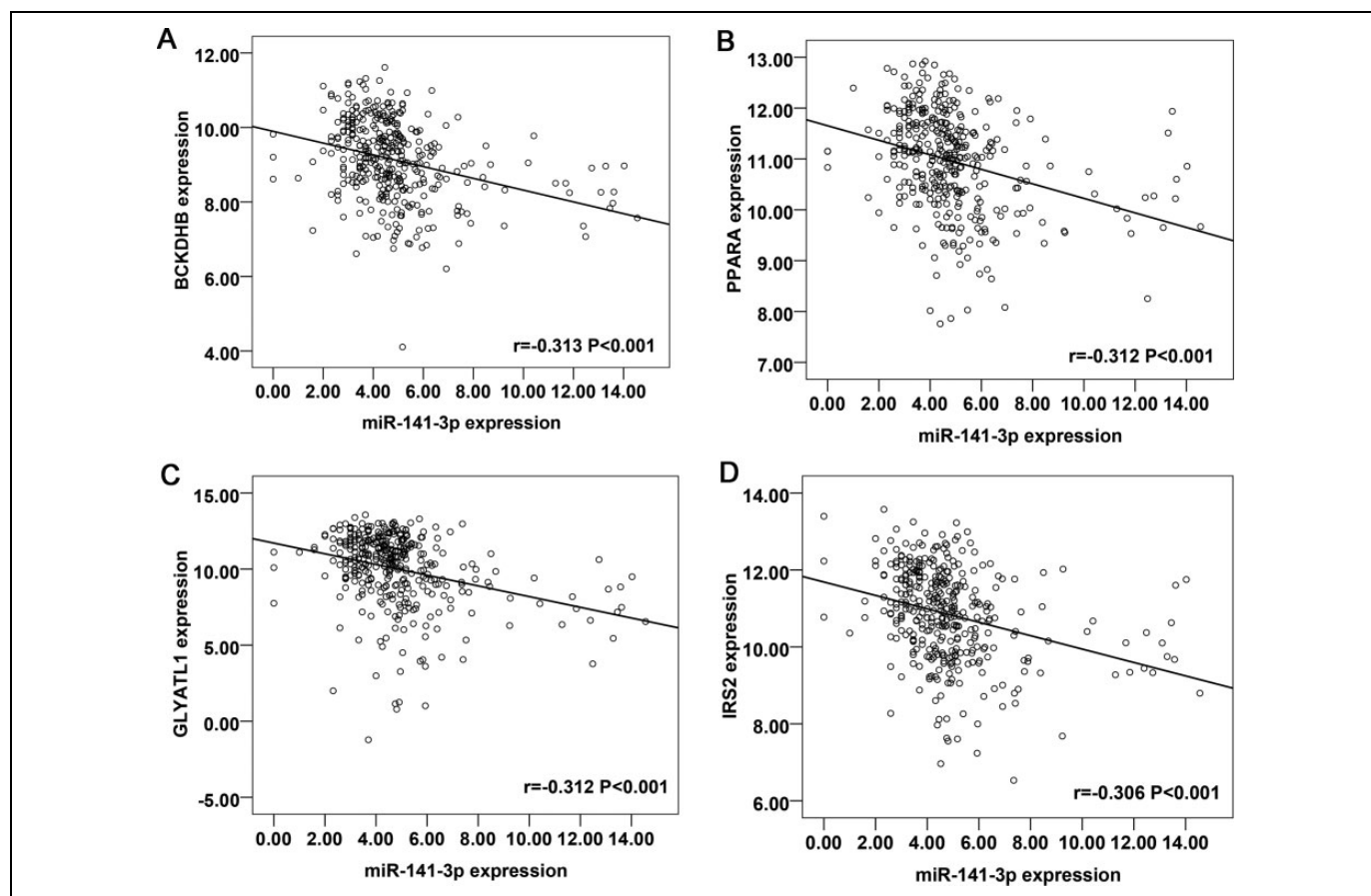


Figure 7. The correlation between miR-141-3p and 4 identified targets. A, BCKDHB ($r = -.313$, $P < .001$). B, PPARA ($r = -.312$, $P < .001$). C, GLYATL1 ($r = -.312$, $P < .001$). D, IRS2 ($r = -.306$, $P < .001$). BCKDHB, branched chain keto acid dehydrogenase E1 subunit beta; PPARA, peroxisome proliferator activated receptor alpha; GLYATL1, glycine-N-acyltransferase like 1; IRS2, insulin receptor substrate 2.

Table 3. The GO Analysis of the Overlap Between Predicted Target Genes, Validated Targets of miR-141-3p, and NLP.^a

| GO ID | Term | Count | P Value |
|---------|--|-------|----------|
| | Biological process | | |
| 0042127 | Regulation of cell proliferation | 61 | 8.65E-21 |
| 0008284 | Positive regulation of cell proliferation | 40 | 1.16E-16 |
| 0007167 | Enzyme-linked receptor protein signaling pathway | 35 | 2.95E-15 |
| 0007169 | Transmembrane receptor protein tyrosine kinase signaling pathway | 27 | 1.81E-13 |
| 0010033 | Response to organic substance | 46 | 2.02E-12 |
| | Cellular component | | |
| 0031974 | Membrane-enclosed lumen | 62 | 5.31E-07 |
| 0043233 | Organelle lumen | 61 | 6.16E-07 |
| 0005654 | Nucleoplasm | 35 | 1.21E-05 |
| 0031981 | Nuclear lumen | 48 | 2.24E-05 |
| 0070013 | Intracellular organelle lumen | 55 | 3.06E-05 |
| | Molecular function | | |
| 0004714 | Transmembrane receptor protein tyrosine kinase activity | 13 | 6.38E-06 |
| 0004713 | Protein tyrosine kinase activity | 18 | 2.12E-05 |
| 0004672 | Protein kinase activity | 32 | 3.55E-05 |
| 0019899 | Enzyme binding | 29 | 3.82E-05 |
| 0005021 | Vascular endothelial growth factor receptor activity | 5 | 6.26E-05 |

Abbreviations: GO, gene ontology; NLP, natural language processing.

^aIn the GO analysis of the overlap between NLP and predicted target genes of miR-141-3p, there were 489 available biological processes, 33 cellular components, and 59 molecular functions ($P < .05$). In this table, the first 5 terms of the GO analysis were shown.

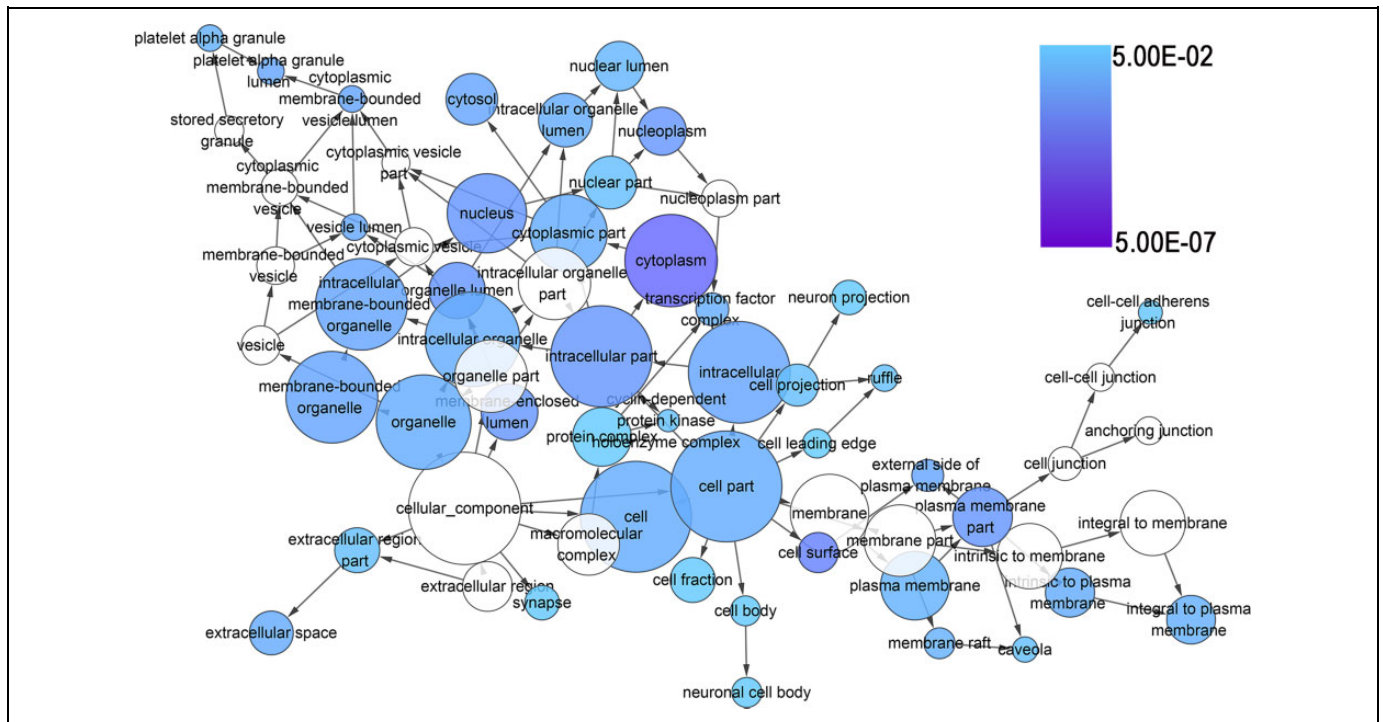


Figure 9. The BINGO analysis network: CC. Each node represents a biological process. A larger node means that more genes are participating in the process. All colored nodes indicate statistical significance ($P < .05$). The deeper color indicates a smaller P value for the biological process. White-colored nodes were used to connect the biological processes without statistical significance. CC indicates cellular components. BINGO, Biological Networks Gene Ontology.

miR-141-3p expression in various cancers. Therefore, it is vital to understand the aberrant expression of miR-141-3p in HCC.

There have been only 2 studies that focused on miR-141-3p expression in HCC tissues.^{9,10} Xue *et al* demonstrated that miR-141-3p was underexpressed in 20 HCC tissues compared to 20 corresponding healthy control tissues.¹⁰ Liu *et al* discovered that miR-141-3p was downregulated in 30 HCC tissues compared to 30 adjacent nontumor samples.⁹ According to the 2 aforementioned studies, miR-141-3p expression may be lower in HCC. However, these 2 studies were conducted on small sample sizes, which reduced its reliability. Therefore, further validation of miR-141-3p expression levels in HCC is necessary.

In this current study, we concentrated on miR-141-3p expression in HCC with clinical parameters. Although the meta-analysis based on the microarray data from the GEO showed a negative result ($P = .984$), we observed a striking reduction miR-141-3p levels in 49 HCC tissues compared to the 49 matched adjacent normal liver tissues in the TCGA database ($P = .045$). The consistent trend was verified by qRT-PCR (95 pairs, $P = .001$), and the results were in accordance with the results of Xue *et al* and Liu *et al*. Our conclusion, which focused on miR-141-3p expression in HCC, was drawn from the larger sample size and might be more stable and convincing. Moreover, miR-141-3p might be a potential biomarker for HCC diagnosis due to the AUC values of 0.647 in TCGA data ($P = .003$) and

0.677 in the qRT-PCR validation ($P < .001$). In other words, the results above confirmed the aberrant expression of miR-141-3p in HCC and its clinical value for HCC diagnosis. However, further *in vivo* and *in vitro* investigations are required to clarify the relative mechanisms of alterations in miR-141-3p expression in HCC.

Concerning the clinicopathological characteristics of the development of HCC, such as tumor nodes, metastasis, and TNM stage, we noticed that these clinicopathological factors were negatively correlated with the expression of miR-141-3p. Not surprisingly, several studies have identified various regulatory mechanisms involved in the progression of HCC. Lou *et al* confirmed that miR-141-3p could influence cell growth and metastasis in HCC through the JNK (c-Jun NH2-terminal kinase) pathway.²³ Consistent with these results, Liu *et al* found that miR-141-3p could inhibit migration and invasion by targeting Tiam1.⁹ Moreover, several other targets of miR-141-3p including ZEB2, which is related to cell apoptosis, proliferation, and invasion, were confirmed to be vital to carcinogenesis and the progression of HCC.²⁴⁻²⁶ Altogether, miR-141-3p may play an antioncogene role in HCC.

To further clarify the potential mechanisms of miR-141-3p in carcinogenesis and the progression of HCC, a gene functional enrichment analysis was performed. In the gene functional enrichment analysis, the NLP analysis was responsible for the HCC-related genes, and the 12 prediction databases and 3 databases for validated targets embodied the miR-141-3p

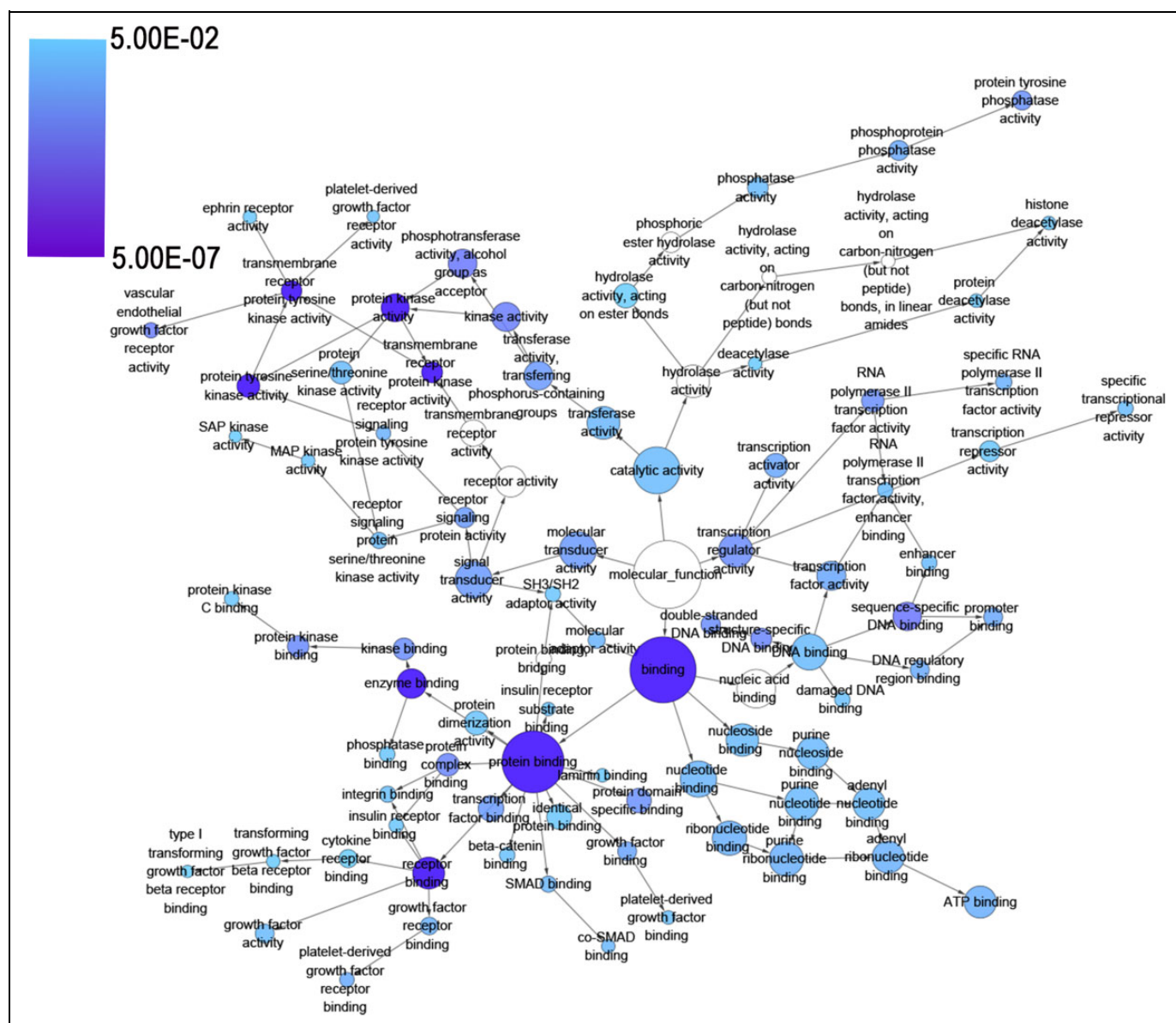


Figure 10. The BINGO analysis network: MF. Each node represents a biological process. A larger node means that more genes are participating in the process. All colored nodes indicate statistical significance ($P < .05$). The deeper color indicates a smaller P value for the biological process. White-colored nodes were used to connect the biological processes without statistical significance. MF indicates molecular functions. BINGO, Biological Networks Gene Ontology.

target genes. After combining the 3 analyses, the overlapping genes were identified as genes that might be involved in the regulatory mechanisms of miR-141-3p in HCC. The protein–protein network of the overlapping genes revealed several hub genes, including PTEN, SRC, PRKCA, PTGS2, and so on. In the Pearson correlative analysis, 7 targets of miR-141-3p showed relatively higher correlation with miR-141-3p (CES2, MYRIP, PEBP1, BCKDHB, PPARA, GLYATL1, and IRS2). However, the bioinformatics analysis for identifying targets may produce results with weak evidence. Thus, whether these identified targets of miR-141-3p in HCC were involved in the pathogenesis of HCC needs further validation in future studies. Further *in vivo* and *in vitro* experiments are needed to

confirm the relationships between miR-141-3p and its identified targets in HCC, especially the hub genes in protein–protein network and the well-correlated targets in Pearson correlative analysis. In the GO analysis of the overlapping genes, some of the target genes were correlated with the regulation of cell proliferation, the enzyme–linked receptor protein signaling pathway, and protein tyrosine kinase activity. These relative functions of the overlapping genes may be essential to the pathogenesis and progression of HCC.^{27,28} Further experiments are also necessary to demonstrate the functions of these target genes.

In the pathway analysis, we obtained 34 significant signaling pathways in the KEGG database and 13 noteworthy

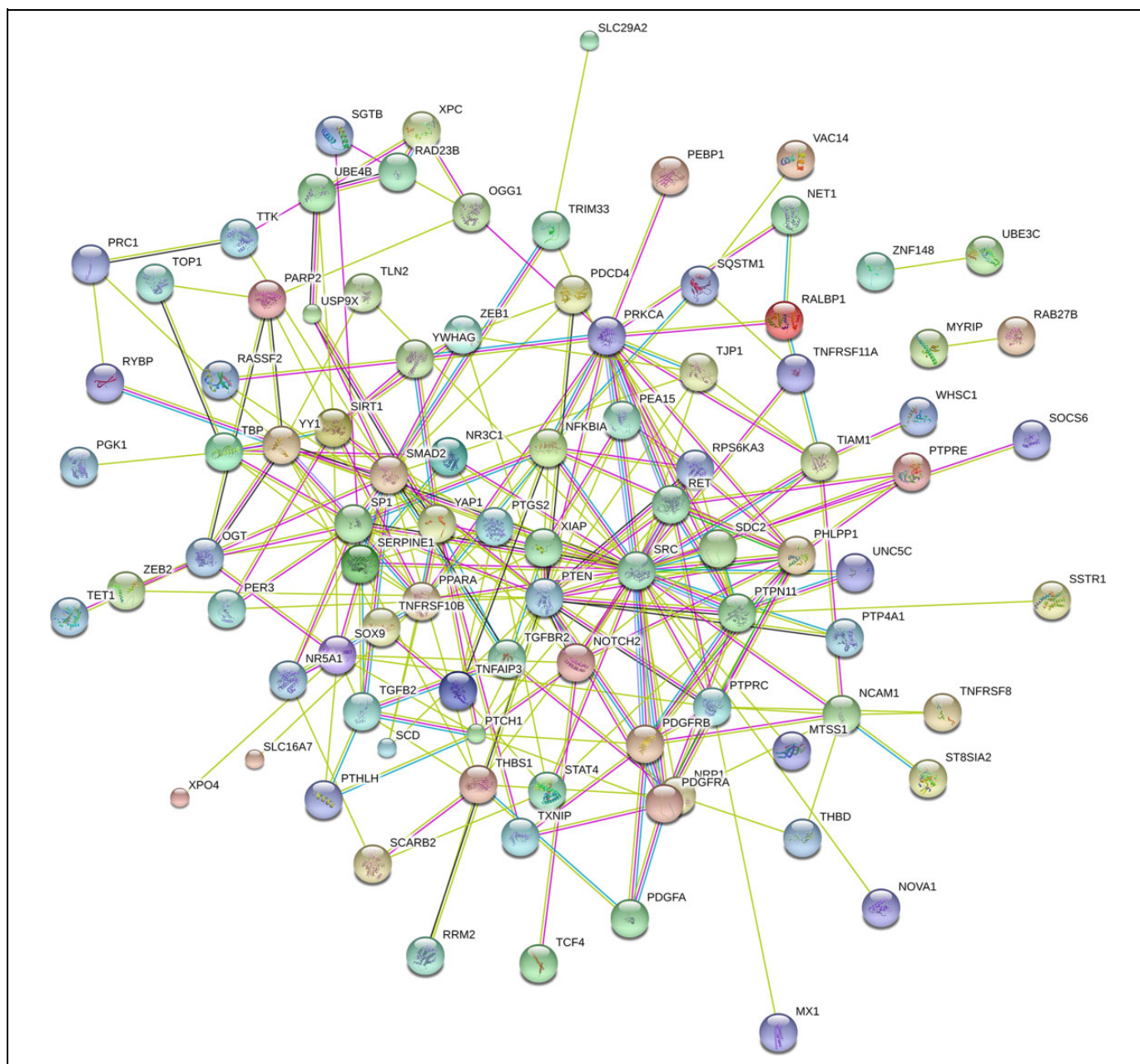


Figure 11. Protein–protein interaction of the overlapping genes between the predicted target genes of miR-141-3p and the NLP analysis. The protein-to-protein network analysis of the 178 overlapping genes of the predicted targets of miR-141-3p and the NLP analysis was performed using the STRING website. The nodes represent proteins, and each color corresponds to a cluster. The edges indicate the predicted functional associations, which are colored according to the types of predicted associations using different sets of evidence. The red, green, blue, purple, yellow, light blue, and black lines indicate fusion evidence, neighborhood evidence, co-occurrence evidence, experimental evidence, text-mining evidence, database evidence, and coexpression evidence, respectively. The line thickness indicates the strength of the evidence. NLP indicates natural language processing. STRING, search tool for recurring instances of neighbouring genes.

signaling pathways of the overlapping genes, including the MAPK signaling pathway, the p53 signaling pathway, and the EGFR signaling pathway. Among them, several dysfunctional signaling pathways have been shown to contribute to oncogenesis and the progression of HCC.²⁸⁻³⁰ Further *in vitro* and *in vivo* investigations of miR-141-3p functions in those signaling pathways in HCC are necessary to confirm and clarify the regulatory mechanisms of miR-141-3p in HCC.

In conclusion, miR-141-3p may play a tumor-suppressing role in the pathogenesis and development of HCC through the regulation of cell proliferation, the enzyme–linked receptor protein signaling pathway, protein tyrosine kinase activity, and several important pathways involved in carcinogenesis and progression, including the MAPK signaling pathway, the p53 signaling pathway, and the EGFR signaling pathway. Further investigations are necessary to confirm the relationships

Table 4. Pathway Analysis of the Overlap of NLP Analysis, Predicted Target Genes, and Validated Targets of miR-141-3p in KEGG.^a

| Title | Count | P Value | Genes |
|------------------------------------|-------|----------|--|
| hsa05200: Pathways in cancer | 38 | 1.45E-12 | FGFR1, E2F3, PTGS2, XIAP, GRB2, PDGFA, NFKBIA, KITLG, GLI2, PTEN, TGFB2, CCNE2, KRAS, ITGAV, AXIN1, EGFR, PRKCA, RET, CTBP2, RALBP1, MSH2, CBL, TGFB2, CYCS, CDK6, SMAD2, HGF, CTNNA1, CDK2, MAPK1, CRKL, CDKN1B, HDAC2, ITGA6, PDGFRA, MAPK9, PDGFRB, PTCH1 |
| hsa05220: Chronic myeloid leukemia | 14 | 3.41E-07 | E2F3, CTBP2, GRB2, CBL, TGFB2, NFKBIA, CDK6, PTPN11, TGFB2, MAPK1, CRKL, HDAC2, CDKN1B, KRAS |
| hsa05215: Prostate cancer | 15 | 4.12E-07 | EGFR, FGFR1, E2F3, PDGFA, GRB2, CREB1, NFKBIA, PTEN, CDK2, CCNE2, MAPK1, CDKN1B, KRAS, PDGFRA, PDGFRB |
| hsa04115: p53 signaling pathway | 12 | 5.74E-06 | E2F1, FGF19, MAPK1, E2F3, BRAF, CDK6, CDK4, FGF2, PTEN, AKT2 |
| hsa05210: Colorectal cancer | 13 | 8.14E-06 | E2F1, CDC42, MAPK1, E2F3, BRAF, RAC1, CDK6, CDK4, FIGF, AKT2 |
| hsa04510: Focal adhesion | 20 | 1.06E-05 | PRKCA, E2F1, MAPK1, E2F3, BRAF, CDK6, CDK4, PTEN, AKT2 |
| hsa04012: ErbB signaling pathway | 13 | 1.18E-05 | PRKCA, CDC42, MAPK1, CAV1, FLT1, BRAF, XIAP, CCND2, BCL2, ITGAV, RAC1, FIGF, PTEN, FN1, AKT2 |
| hsa05214: Glioma | 11 | 1.85E-05 | E2F1, E2F3, XIAP, BCL2, ITGAV, CDK6, CDK4, PTEN, FN1, AKT2 |
| hsa04010: MAPK signaling pathway | 23 | 1.88E-05 | PRKCA, E2F1, MAPK1, E2F3, BRAF, CDK6, CDK4, AKT2 |
| hsa04110: Cell cycle | 15 | 2.52E-05 | E2F1, MAPK1, E2F3, BRAF, CDK4, FIGF, MMP2 |

Abbreviations: KEGG, Kyoto Encyclopedia of Genes and Genomes; MAPK1, Mitogen-Activated Protein Kinase 1; NLP, natural language processing.

^aThe pathway analysis was performed in KEGG database, and there were 39 available pathways. Among them, 34 signaling pathways were significant ($P < .05$), and the top 10 pathways are shown in this table.

Table 5. Pathway Analysis of the Overlap of NLP Analysis, Predicted Target Genes, and Validated Targets of miR-141-3p in Panther.^a

| Title | Count | P Value | Genes |
|---|-------|-------------|--|
| P00005: Angiogenesis | 23 | 2.60E-05 | PRKCA, FGFR1, PDGFA, GRB2, MAP2K4, JAG1, SRC, EPHB1, PTPN11, KDR, NOTCH2, MAPK1, STAT4, EPHA7, CRKL, KRAS, MAPK14, ARHGAP1, PDGFRA, MAPK9, PDGFRB, FRS2, AXIN1 |
| P00059: p53 pathway | 14 | 6.00E-04 | E2F3, CCNG1, CDC25C, PTEN, SIRT1, ATM, CDK2, CDC25A, CCNE2, YWHAG, HDAC2, TNFRSF10B, SERPINE1, THBS1 |
| P00018: EGF receptor signaling pathway | 15 | 8.93E-04 | PRKCA, EGFR, ERBB4, GRB2, CBL, MAP2K4, ATM, MAPK1, YWHAG, STAT4, KRAS, MAPK14, MAPK9, PEBP1, MAP2K7 |
| P00048: PI3 kinase pathway | 13 | 0.001374803 | IRS2, FOXA2, GNAI1, FOXJ1, GRB2, FOXO3, PTEN, FOXP1, YWHAG, KRAS, CCND2, FOXC1, INSR |
| P00021: FGF signaling pathway | 13 | 0.00503131 | PRKCA, FGFR1, GRB2, MAP2K4, PTPN11, MAPK1, YWHAG, KRAS, MAPK14, MAPK9, PEBP1, MAP2K7, FRS2 |
| P04393: Ras pathway | 10 | 0.007341781 | MAPK1, RPS6KA3, STAT4, KRAS, TIAM1, GRB2, MAPK14, MAP2K4, MAPK9, MAP2K7 |
| P00032: Insulin/IGF pathway-mitogen-activated protein kinase/MAP kinase cascade | 7 | 0.008789569 | MAPK1, RPS6KA3, IRS2, GRB2, MAP2K4, MAP2K7, INSR |
| P04398: p53 pathway feedback loops 2 | 8 | 0.009289086 | CCNE2, E2F3, KRAS, MAPK14, CCNG1, PTEN, ATM, CDK2 |
| P00006: Apoptosis signaling pathway | 11 | 0.026283102 | PRKCA, ATF6, MAPK1, TNFRSF10B, XIAP, CREB1, CYCS, MAP2K4, NFKBIA, MAPK9, MAP2K7 |
| P00052: TGF- β signaling pathway | 12 | 0.033037544 | MAPK1, KRAS, FOXA2, FOXJ1, MAPK14, TGFB2, MAPK9, SMAD2, FOXC1, FOXO3, FOXP1, TGFB2 |

Abbreviations: EGF, epidermal growth factor; FGF, fibroblast growth factor; IGF, insulin-like growth factor; MAP, mitogen-activated protein; NLP, natural language processing; TGF, transforming growth factor.

^aThis pathway analysis was performed in Panther database, and there were 16 available pathways. Among them, 13 signaling pathways were significant ($P < .05$), and the top 10 pathways are shown in this table.

between miR-141-3p and certain key hub genes (PTEN, SRC, PRKCA, and PTGS2) in the pathogenesis of HCC. Thus, interactions with miR-141-3p may supply an original viewpoint for HCC treatment.

Declaration of Conflicting Interests

The author(s) declared no potential conflicts of interest with respect to the research, authorship, and/or publication of this article.

Funding

The author(s) received no financial support for the research, authorship, and/or publication of this article.

References

- Chen W, Zheng R, Baade PD, et al. Cancer statistics in China, 2015. *CA Cancer J Clin.* 2016;66(2):115-32. doi:10.3322/caac.21338. PubMed PMID: 26808342.
- Siegel RL, Miller KD, Jemal A. Cancer statistics, 2016. *CA Cancer J Clin.* 2016;66(1):7-30. doi:10.3322/caac.21332. PubMed PMID: 26742998.
- Park SH, Kim JC, Kang MK. Technical advances in external radiotherapy for hepatocellular carcinoma. *World J Gastroenterol.* 2016;22(32):7311-7321. doi:10.3748/wjg.v22.i32.7311. PubMed PMID: 27621577; PubMed Central PMCID: PMC4997637.
- Ohri N, Kaubisch A, Garg M, Guha C. Targeted therapy for hepatocellular carcinoma. *Semin Radiat Oncol.* 2016;26(4):338-343. doi:10.1016/j.semradonc.2016.06.004. PubMed PMID: 27619254.
- Liu LN, Li DD, Xu HX, Zheng SG, Zhang XP. Role of microRNAs in hepatocellular carcinoma. *Front Biosci.* 2015;20:1056-1067. PubMed PMID: 25961544.
- Wang Y, Sun B, Sun H, et al. Regulation of proliferation, angiogenesis and apoptosis in hepatocellular carcinoma by miR-26b-5p. *Tumour Biol.* 2016;37(8):10965-10979. doi:10.1007/s13277-016-4964-7. PubMed PMID: 26891666.
- Zhou X, Zhang L, Zheng B, et al. MicroRNA-761 is upregulated in hepatocellular carcinoma and regulates tumorigenesis by targeting Mitofusin-2. *Cancer Sci.* 2016;107(4):424-432. doi:10.1111/cas.12904. PubMed PMID: 26845057; PubMed Central PMCID: PMC4832850.
- Li WF, Dai H, Ou Q, Zuo GQ, Liu CA. Overexpression of microRNA-30a-5p inhibits liver cancer cell proliferation and induces apoptosis by targeting MTDH/PTEN/AKT pathway. *Tumour Biol.* 2016;37(5):5885-5895. doi:10.1007/s13277-015-4456-1. PubMed PMID: 26589417.
- Liu Y, Ding Y, Huang J, et al. MiR-141 suppresses the migration and invasion of HCC cells by targeting Tiam1. *PLoS One.* 2014;9(2):e88393. doi:10.1371/journal.pone.0088393. PubMed PMID: 24551096; PubMed Central PMCID: PMC3923786.
- Xue J, Niu YF, Huang J, et al. miR-141 suppresses the growth and metastasis of HCC cells by targeting E2F3. *Tumour Biol.* 2014;35(12):12103-12107. doi:10.1007/s13277-014-2513-9. PubMed PMID: 25142234.
- Ioannidis JP, Patsopoulos NA, Evangelou E. Uncertainty in heterogeneity estimates in meta-analyses. *BMJ.* 2007;335(7626):914-916. doi:10.1136/bmj.39343.408449.80. PubMed PMID: 17974687; PubMed Central PMCID: PMC2048840.
- Huang WT, Wang HL, Yang H, et al. Lower expressed miR-198 and its potential targets in hepatocellular carcinoma: a clinico-pathological and in silico study. *Onco Targets Ther.* 2016;9:5163-5180. doi:10.2147/OTT.S108828. PubMed PMID: 27578984; PubMed Central PMCID: PMC5001667.
- Huang WT, Chen ZX, He RQ, et al. Clinicopathological role of miR-30a-5p in hepatocellular carcinoma tissues and prediction of its function with bioinformatics analysis. *Onco Targets Ther.* 2016;9:5061-5071. doi:10.2147/OTT.S111431. PubMed PMID: 27574447; PubMed Central PMCID: PMC4990378.
- Tang R, Liang L, Luo D, et al. Downregulation of MiR-30a is associated with poor prognosis in lung cancer. *Med Sci Monit.* 2015;21:2514-2520. doi:10.12659/MSM.894372. PubMed PMID: 26305739; PubMed Central PMCID: PMC4554363.
- Dweep H, Gretz N. miRWalk2.0: a comprehensive atlas of microRNA-target interactions. *Nat Methods.* 2015;12(8):697. doi:10.1038/nmeth.3485. PubMed PMID: 26226356.
- Huang da W, Sherman BT, Lempicki RA. Systematic and integrative analysis of large gene lists using DAVID bioinformatics resources. *Nat Protoc.* 2009;4(1):44-57. doi:10.1038/nprot.2008.211. PubMed PMID: 19131956.
- Szklarczyk D, Franceschini A, Wyder S, et al. STRING v10: protein-protein interaction networks, integrated over the tree of life. *Nucleic Acids Res.* 2015;43(Database issue):D447-D452. doi:10.1093/nar/gku1003. PubMed PMID: 25352553; PubMed Central PMCID: PMC4383874.
- Behbahani GD, Ghahhari NM, Javidi MA, Molan AF, Feizi N, Babashah S. MicroRNA-mediated post-transcriptional regulation of epithelial to mesenchymal transition in cancer. *Pathol Oncol Res.* 2017;23(1):1-12. doi:10.1007/s12253-016-0101-6. PubMed PMID: 27590333.
- Xu F, He H, Huang W, et al. Decreased expression of MicroRNA-200 family in human breast cancer is associated with lymph node metastasis. *Clin Transl Oncol.* 2016;18(3):283-288. doi:10.1007/s12094-015-1364-1. PubMed PMID: 26201425.
- Chang L, Guo F, Huo B, Lv Y, Wang Y, Liu W. Expression and clinical significance of the microRNA-200 family in gastric cancer. *Oncol Lett.* 2015;9(5):2317-2324. doi:10.3892/ol.2015.3028. PubMed PMID: 26137064; PubMed Central PMCID: PMC4467351.
- Mei Z, He Y, Feng J, et al. MicroRNA-141 promotes the proliferation of non-small cell lung cancer cells by regulating expression of PHLPP1 and PHLPP2. *FEBS Lett.* 2014;588(17):3055-3061. doi:10.1016/j.febslet.2014.06.020. PubMed PMID: 24945731.
- Mahdavinzhad A, Mousavi-Bahar SH, Poorolajal J, et al. Evaluation of miR-141, miR-200c, miR-30b expression and clinico-pathological features of bladder cancer. *Int J Mol Cell Med.* 2015;4(1):32-39. PubMed PMID: 25815280; PubMed Central PMCID: PMC4359703.
- Lou G, Dong X, Xia C, et al. Direct targeting sperm-associated antigen 9 by miR-141 influences hepatocellular carcinoma cell growth and metastasis via JNK pathway. *J Exp Clin Cancer Res.*

- 2016;35:14. doi:10.1186/s13046-016-0289-z. PubMed PMID: 26790956; PubMed Central PMCID: PMC4721207.
24. Wu SM, Ai HW, Zhang DY, et al. MiR-141 targets ZEB2 to suppress HCC progression. *Tumour Biol.* 2014;35(10):9993-9997. doi: 10.1007/s13277-014-2299-9. PubMed PMID: 25008569.
25. Shi L, Wu L, Chen Z, et al. MiR-141 activates Nrf2-dependent antioxidant pathway via down-regulating the expression of Keap1 conferring the resistance of hepatocellular carcinoma cells to 5-fluorouracil. *Cell Physiol Biochem.* 2015;35(6):2333-2348. doi: 10.1159/000374036. PubMed PMID: 25896253.
26. Lin L, Liang H, Wang Y, et al. microRNA-141 inhibits cell proliferation and invasion and promotes apoptosis by targeting hepatocyte nuclear factor-3beta in hepatocellular carcinoma cells. *BMC Cancer.* 2014;14:879. doi:10.1186/1471-2407-14-879. PubMed PMID: 25425543; PubMed Central PMCID: PMC4289273.
27. Swamy SG, Kameshwar VH, Shubha PB, et al. Targeting multiple oncogenic pathways for the treatment of hepatocellular carcinoma. *Target Oncol.* 2017;12(1):1-10. doi:10.1007/s11523-016-0452-7. PubMed PMID: 27510230.
28. Zhan L, Cao H, Wang G, et al. Drp1-mediated mitochondrial fission promotes cell proliferation through crosstalk of p53 and NF-kappaB pathways in hepatocellular carcinoma. *Oncotarget.* 2016;7(40):65001-65011. doi:10.18632/oncotarget.11339. PubMed PMID: 27542250.
29. Li H, Miao Q, Xu CW, Huang JH, Zhou YF, Wu MJ. OTX1 contributes to hepatocellular carcinoma progression by regulation of ERK/MAPK pathway. *J Korean Med Sci.* 2016;31(8):1215-1223. doi:10.3346/jkms.2016.31.8.1215. PubMed PMID: 27478331; PubMed Central PMCID: PMC4951550.
30. Huang S, He R, Rong M, Dang Y, Chen G. Synergistic effect of MiR-146a mimic and cetuximab on hepatocellular carcinoma cells. *Biomed Res Int.* 2014;2014:384121. doi:10.1155/2014/384121. PubMed PMID: 24895573; PubMed Central PMCID: PMC4033429.